Direct Torque Control Schemes for Split-phase Induction Machine

*Kamalesh Hatua, V.T. Ranganathan

* *Present Address*: Honeywell Technology Solutions Lab Pvt. Ltd.
Bannerghatta Road,
Bangalore -- 560 076, India.
e-mail: kamalesh.hatua@honeywell.com,

Power Electronics Group, Dept.of Electrical Engineering,
Indian Institute of Science,
Bangalore -- 560 012, India
e-mail: vtran@ee.iisc.ernet.in

***Abstract* – In this paper, DTC (Direct Torque Control) algorithms for Split-phase Induction Machine (SPIM) are established. SPIM has two sets of three-phase stator windings, with a shift of thirty electrical degrees between them. The significant contributions of the present work are: a) Two new methods of DTC technique for SPIM are developed. They are called as Resultant Flux Control Method and Individual Flux Control Method. b) Advantages and disadvantages of both the methods are discussed. High torque ripple is a disadvantage for three-phase DTC. It is found that torque ripple in SPIM could be significantly reduced without increasing the switching frequency.**

***Keywords* – SPIM, DTC, Resultant Flux Control Method, Individual Flux Control Method**

I. INTRODUCTION

In early eighties, current source inverters (CSI) were used to drive the induction machines. Due to lower switching frequency of operation, sixth harmonic torque pulsations were predominant. Sixth harmonic torque pulsations are produced mainly due to the interaction between the fundamental flux and the fifth and seventh harmonic rotor currents. To eliminate sixth harmonic torque pulsations, split phase induction machine (SPIM), structure was proposed. SPIM has two sets of three-phase winding. In this configuration, sixth harmonic torque pulsations produced by the two sets of windings are in phase opposition. So sixth harmonic torque pulsations are completely absent in SPIM. Afterwards SPIM was operated with two independent voltage source inverters[2]. Due to advent of IGBT, inverters are switched at much higher frequency than fundamental. So low order harmonics are practically absent in induction machine drive. Therefore, today sixth harmonic torque pulsations are not an issue. However, the SPIM configuration can still offer many attractive features, some of which are:

a) Applying nearly half the rated voltage of original three-phase machine, to each half winding, full flux linkage can be established in the SPIM. This feature favors applications in high power, traction and electric vehicles.

b) M.m.f profile is smoother in SPIM compared to three-phase induction machine.

c) Control options are more in SPIM, compared to three-phase induction machine. In this paper, control options of SPIM are used properly to establish the DTC technique. It was found, that torque ripple can be reduced significantly in SPIM.

II. STRUCTURE OF SPIM DRIVE

When the phase belt of a three-phase induction machine with even number of slots per pole per phase is split into two equal halves, a SPIM results with two sets of stator coils with their axes separated by thirty-electrical degrees (Fig. 1)[2]. The supply to A2B2C2 winding group is thirty-degree phase advanced from that of A1B1C1 winding group. When SPIM is operated in this fashion, then individual m.m.fs generated from each set of windings will algebraically add up to generate resultant m.m.f. If any 5^{th} and 7^{th} harmonic components are present in the voltage, they will not generate any 5^{th} and 7^{th} harmonic rotor currents due to split winding pattern. Practically sixth harmonic torque pulsations can be avoided in this machine. In the present DTC schemes, two independent two-level voltage source inverters drive the machine. They share a common D.C. bus (Fig.2). Neutrals of both sets of windings are kept isolated. Since there are two independent three-phase inverters driving the SPIM, there are a total of 49 (7X7) voltage space phasor locations possible. All active space phasor locations can be viewed as four concentric twelve-sided polygons (Fig.3).

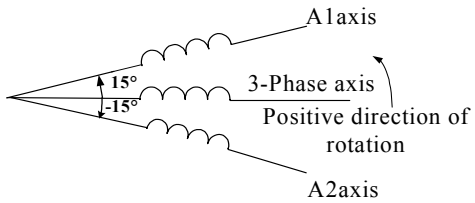

Fig.1. Machine winding

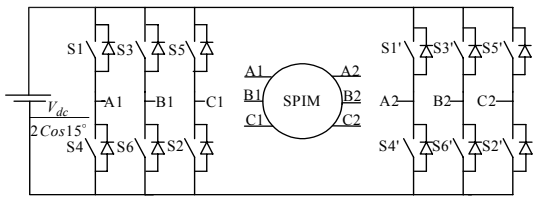

Fig.2. SPIM Drive

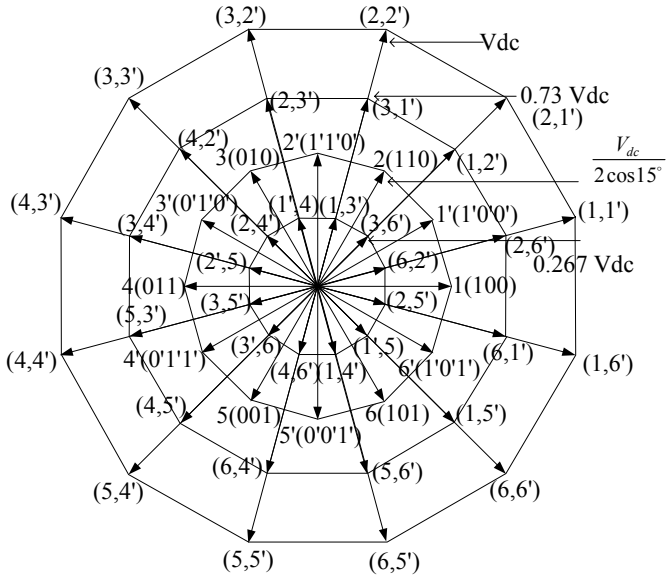

Fig.3. Space vectors for SPIM drive

The vector locations of the A1B1C1 phase group are phase shifted by thirty degrees from those of the A2B2C2 phase group. In Fig.3, all possible space phasor locations are shown. The sequence 1',2',3',4',5',6' is that of the A1B1C1 phase group, and the sequence 1,2,3,4,5,6 is that of the A2B2C2 phases [2].

III. PRINCIPLE OF OPERATION

In conventional three-phase DTC algorithm all control parameters are measured in the stationary reference frame commonly known as α-β reference frame [1]. In this reference frame, electromagnetic torque can be expressed as the vector cross product of stator flux and rotor flux. Inverter1 and inverter2 establish stator fluxes $\vec{\Psi}_{s1}$ and $\vec{\Psi}_{s2}$ in the A1B1C1 and A2B2C2 winding respectively. Resultant stator flux ($\vec{\Psi}_{res}$) is space vectorial addition of individual stator fluxes. $\vec{\Psi}_{res}$ is equivalent to three-phase stator flux $\vec{\Psi}_s$. Rotor of SPIM is assumed to be three-phase [2]. Thus the torque of SPIM can also be expressed as vector cross product of $\vec{\Psi}_{res}$ and $\vec{\Psi}_r$, where $\vec{\Psi}_r$ is the rotor flux of SPIM. To control the torque and the flux directly, the main goal of DTC, $\vec{\Psi}_{res}$ is rotated along a circular trajectory, selecting appropriate voltage vectors from both the inverters, similar to three-phase DTC algorithm (Fig.4).

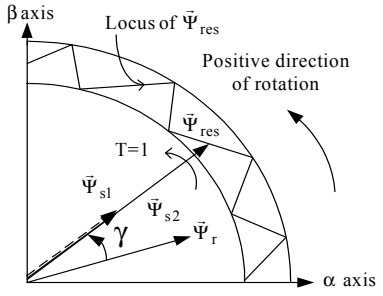

Fig.4. Operating principle for SPIM

IV. SPIM MODEL

DTC is stator side control of ac machines. Estimations of machine torque and stator fluxes are to be calculated from the available state variables and parameters of the machine $\vec{\Psi}_{res}$ is measured from resultant three-phase axis(Fig.1). $\vec{\Psi}_{s1}$ and $\vec{\Psi}_{s2}$ are measured from their own individual axes (Fig.1). Resultant electromagnetic torque (md) can be expressed as the algebraic addition of individual torques (md1 & md2) contributed by both the inverters [4].

$$\vec{\Psi}_{res} = \vec{\Psi}_{s1} e^{j15^\circ} + \vec{\Psi}_{s2} e^{-j15^\circ} \quad (1) \qquad m_d = m_{d1} + m_{d2} \quad (4)$$

$$\vec{\Psi}_{s1} = \int \left(\vec{V}_{s1} - R_{s1} \vec{i}_{s1} \right) dt \quad (2) \qquad m_{d1} = -\frac{2}{3}\frac{P}{2} \left[\vec{\Psi}_{s1} \times \vec{i}_{s1} \right] \quad (5)$$

$$\vec{\Psi}_{s2} = \int \left(\vec{V}_{s2} - R_{s2} \vec{i}_{s2} \right) dt \quad (3) \qquad m_{d2} = -\frac{2}{3}\frac{P}{2} \left[\vec{\Psi}_{s2} \times \vec{i}_{s2} \right] \quad (6)$$

V. RESULTANT FLUX CONTROL METHOD

A total of forty-nine different space phasor combinations are possible in SPIM drive. The outermost locations form a twelve-sided polygon. In this method $\vec{\Psi}_{res}$ is rotated in a circular trajectory, switching the vectors from outermost twelve-sided polygon (Fig.5). As $\vec{\Psi}_{res}$ is rotated in a circular trajectory, it induces sinusoidal voltages and currents in the rotor and the output torque is free from sixth harmonic torque pulsations.

As vectors from the outer twelve-sided polygon are selected, switchings of the inverters are dependent on each other. They cannot be switched independently. But due to these patterns of switching, α and β components of $\vec{\Psi}_{s2}$ lead those of $\vec{\Psi}_{s1}$ by thirty degrees in phase.

Resultant Flux Control Method controls the magnitude of $\vec{\Psi}_{res}$. There is no direct control over individual fluxes. So if pure integration is used to estimate $\vec{\Psi}_{s1}$ and $\vec{\Psi}_{s2}$, they show dc drift tendency. To avoid this problem low pass filter of very low cut-off frequency (1Hz) is used to estimate them [3]. The outermost voltage vectors divide the total trajectory of $\vec{\Psi}_{res}$ into twelve identical sectors (Fig.5). Sector for $\vec{\Psi}_{res}$ is identified by comparing the magnitude of $\Psi_{res\alpha}$ and $\Psi_{res\beta}$.

Three-level torque and two-level flux hysteresis controllers are used as in the case of conventional three-phase DTC [1]. The complete block diagram is shown in fig.6. According to the outputs of the torque controller (1,0,-1), resultant flux controller (1,0) and the sector information (R(N)) of $\vec{\Psi}_{res}$, appropriate voltage vectors for both the inverters are selected from an optimal switching table (table1).

1. T= 1 $\Longrightarrow$ Increase of torque in anti-clockwise direction.
2. T= -1 $\Longrightarrow$ Increase of torque in clockwise direction.
3. T=0 $\Longrightarrow$ Decrease the torque by applying zero vectors.
4. F_{res}=1 $\Longrightarrow$ Increase the magnitude of flux.
4. F_{res}=0 $\Longrightarrow$ Decrease the magnitude of flux.

F_{res}	T	R(1)	R(2)	R(3)	R(4)	R(5)	R(6)	R(7)	R(8)	R(9)	R(10)	R(11)	R(12)
1	**1**	(3,2')	(3,3')	(4,3')	(4,4')	(5,4')	(5,5')	(6,5')	(6,6')	(1,6')	(1,1')	(2,1')	(2,2')
1	**0**	(7,8')	(7,7')	(8,7')	(8,8')	(7,8')	(7,7')	(8,7')	(8,8')	(7,8')	(7,7')	(8,7')	(8,8')
1	**-1**	(6,6')	(1,6')	(1,1')	(2,1')	(2,2')	(3,2')	(3,3')	(4,3')	(4,4')	(5,4')	(5,5')	(6,5')
0	**1**	(3,3')	(4,3')	(4,4')	(5,4')	(5,5')	(6,5')	(6,6')	(1,6')	(1,1')	(2,1')	(2,2')	(3,2')
0	**0**	(7,7')	(8,7')	(8,8')	(7,8')	(7,7')	(8,7')	(8,8')	(7,8')	(7,7')	(8,7')	(8,8')	(7,8')
0	**-1**	(6,5')	(6,6')	(1,6')	(1,1')	(2,1')	(2,2')	(3,2')	(3,3')	(4,3')	(4,4')	(5,4')	(5,5')

Table1

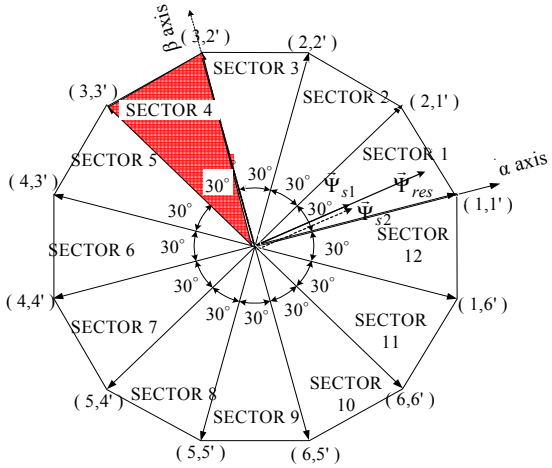

Fig.5. Sector identification

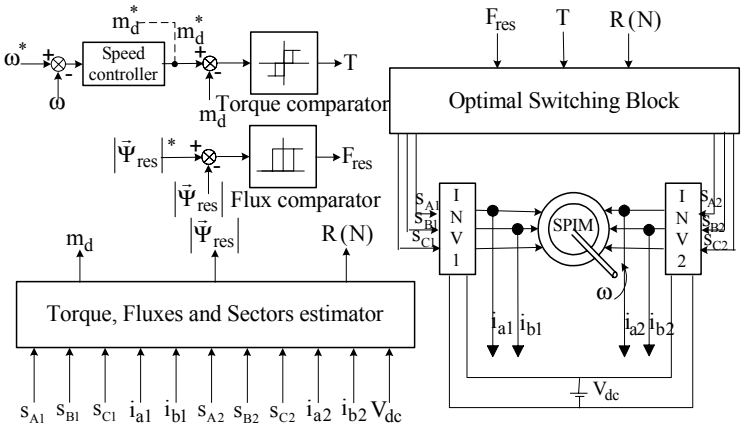

Fig.6.Block diagram for Resultant Flux Control Algorithm

Experimental result: DC Bus:200V,machine speed:570 r.p.m, no load

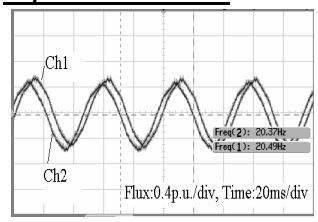

Fig.7.Ch1 : $\Psi_{s\alpha 1}$ Ch2 : $\Psi_{s\alpha 2}$

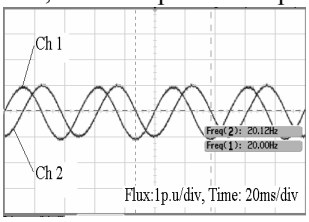

Fig.8.Ch1 : $\Psi_{res\alpha}$ Ch2 : $\Psi_{res\beta}$

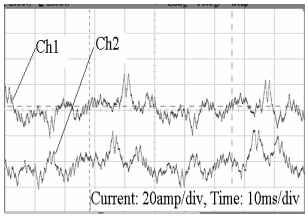

Fig.9.Ch1 : i_{s_a1} Ch2 : i_{s_a2}

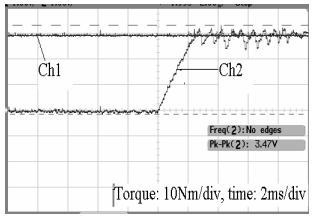

Fig.10.Ch1 : m_d^* Ch2 : m_d

Advantage: a) As the vectors from outermost twelve-sided polygon are used, higher speed range can be achieved with rated flux compared to three-phase DTC [2].

b) For conventional three-phase DTC scheme, angular separation between active voltage vectors and stator flux varies from 90° to 30° or 90° to 150° for positive torque demand. But in this method the variations are from 90° to 60° or 90° to 120°. So the torque response is faster in Resultant Flux Control Method compared to three-phase DTC.

Disadvantage: a) There is no direct control over individual fluxes. So they show dc drift tendency. A low pass filter is used instead of a pure integrator to overcome this problem.

b) $\vec{\Psi}_{s1}$ and $\vec{\Psi}_{s2}$ do not trace pure circular loci like $\vec{\Psi}_{res}$. Therefore both the individual fluxes contain low order harmonics, especially 5^{th} and 7^{th}. In SPIM, 5^{th} and 7^{th} harmonic impedances are very small in magnitude. Thus the machine draws large amount of stator harmonic currents, which in turn increases stator harmonic loss.

VI. INDIVIDUAL FLUX CONTROL METHOD

Individual fluxes are not directly controlled in Resultant Flux Control Method. Therefore the stator currents are rich in low order harmonics especially 5^{th} and 7^{th}. Though they do not cause 6^{th} harmonic torque pulsations due to winding disposition, they result in increased stator losses. To avoid these losses it is required to control individual fluxes directly along with $\vec{\Psi}_{res}$. In Individual Flux Control Method both the inverters are switched from their respective hexagonal space vector locations to maintain the individual and resultant flux magnitudes constant at their respective reference values. Three different algorithms are proposed in this method. These algorithms try to achieve the following goals:

1. Operate SPIM at maximum flux maintaining the phase angle between the components of $\vec{\Psi}_{s1}$ and $\vec{\Psi}_{s2}$ at thirty degrees.
2. Control individual and resultant fluxes in such a way that all of them trace pure circular loci.
3. Reduce resultant torque ripple.

VI.A. BASIC OPERATING PRINCIPLE

During proper SPIM operation, α-β components of $\vec{\Psi}_{s2}$ should lead those of $\vec{\Psi}_{s1}$ by thirty degrees in phase. When the machine is operated in this fashion, both of them add up algebraically and develop maximum resultant flux inside the machine (Fig. 11) [4]. The magnitude of the individual fluxes is half of the rated value of resultant flux.

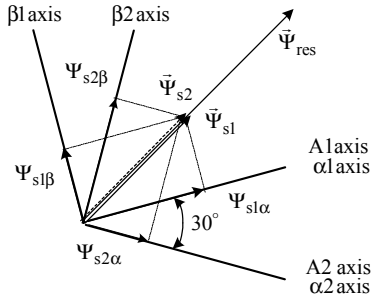

Fig.11. Description of different fluxes

The magnitudes of $\vec{\Psi}_{s1}$ and $\vec{\Psi}_{s2}$ are kept constant at their reference value by two different two-level flux hysteresis controllers. The angle between the components of individual fluxes vary due to different angular velocities of $\vec{\Psi}_{s1}$ and $\vec{\Psi}_{s2}$, inaccuracy in the measurement of currents, fluxes and individual torque contributions of both sets of windings. Therefore the magnitude of $\vec{\Psi}_{res}$ also varies. The magnitude of $\vec{\Psi}_{res}$ is controlled at every instant by controlling the angle between components of $\vec{\Psi}_{s1}$ and $\vec{\Psi}_{s2}$ .To achieve this a fictitious flux $\vec{\Psi}_{res\_t}$ is defined. $\vec{\Psi}_{res\_t}$ does not have any physical significance but its magnitude is used for control action of different Individual Flux Control Algorithms. $\vec{\Psi}_{res\_t}$ is direct addition of $\vec{\Psi}_{s1}$ and $\vec{\Psi}_{s2}$, without transforming them to a common axis (Eq.7).

$$\vec{\Psi}_{res\_t} \triangleq \vec{\Psi}_{s1} + \vec{\Psi}_{s2} \tag{7}$$

If, θ is the angle between the components of $\vec{\Psi}_{s1}$ and $\vec{\Psi}_{s2}$, then the magnitude of $\vec{\Psi}_{res\_t}$ is defined in Equation 9.

$$\left|\vec{\Psi}_{s1}\right|^* = \left|\vec{\Psi}_{s2}\right|^* = \left|\vec{\Psi}_{s2}\right|^* = \frac{1}{2}\left|\vec{\Psi}_{res}\right|^* \tag{8}$$

$$\left|\vec{\Psi}_{res\_t}\right| = 2\cos\theta\left|\vec{\Psi}_{s}\right|^* = \cos\theta\left|\vec{\Psi}_{res}\right|^* \tag{9}$$

The magnitude of $\vec{\Psi}_{res\_t}$ identifies θ (Eq.8-Eq.12), Fig.(12).

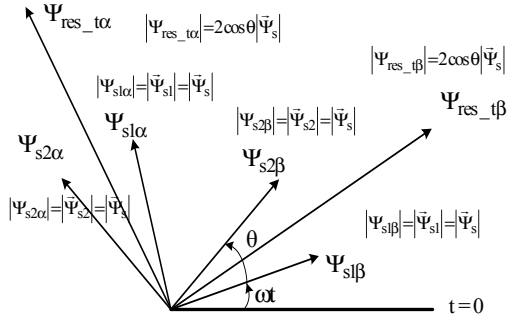

Fig.12. Description of different phasors

$$\left|\vec{\Psi}_{res\_t}\right|^* = 2\cos 15^\circ \left|\vec{\Psi}_{s}\right|^* = \cos 15^\circ \left|\vec{\Psi}_{res}\right|^* \tag{10}$$

$$\left|\vec{\Psi}_{res\_t}\right| < \left|\vec{\Psi}_{res\_t}\right|^* \Rightarrow \theta > 30^\circ \tag{11}$$

$$\left|\vec{\Psi}_{res\_t}\right| > \left|\vec{\Psi}_{res\_t}\right|^* \Rightarrow \theta < 30^\circ \tag{12}$$

Automatically a question arises: why is the magnitude of $\vec{\Psi}_{res}$ not used instead of $\vec{\Psi}_{res\_t}$ to identify the phase angle separation between the components of $\vec{\Psi}_{s1}$ and $\vec{\Psi}_{s2}$?

When , $\theta > 30^\circ$, $\left|\vec{\Psi}_{res}\right| < \left|\vec{\Psi}_{res}\right|^*$ (13)

When, $\theta < 30^\circ$, $\left|\vec{\Psi}_{res}\right| < \left|\vec{\Psi}_{res}\right|^*$ (14)

Hence, whether θ is more or less from the reference value, cannot be judged by the magnitude of $\vec{\Psi}_{res}$, because for both the cases it is less than the reference value.

VII. INDIVIDUAL FLUX CONTROL ALGORITHM #01

In this algorithm, both the inverters are switched from their own hexagonal space vector locations (Fig.13). Magnitudes of individual fluxes are kept constant by conventional two-level flux hysteresis controllers [1]. Sectors of individual fluxes are identified as in conventional three-phase DTC (Fig.13)[1]. A three-level torque hysteresis controller, same as conventional three-phase DTC, controls the magnitude of the resultant torque. During this time θ is kept at thirty degrees by a two-level angle controller (Fig.14).

Torque, Individual fluxes are estimated as discussed in section VI (SPIM model). Pure integrators are used to estimate individual fluxes as hysteresis controllers always control the magnitude of them.

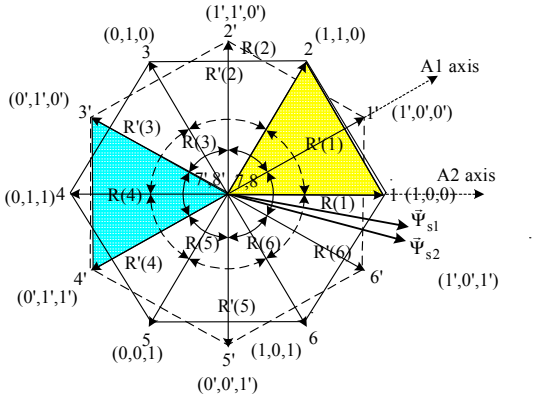

Fig.13.Sector identification

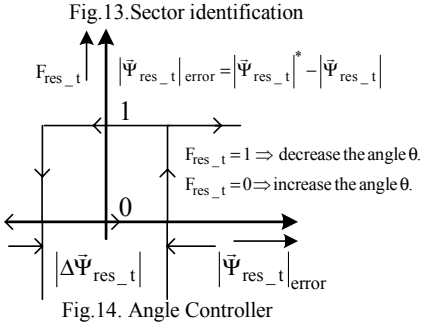

Fig.14. Angle Controller

Optimal switching logic: Two individual switching blocks contain switching signals for the two inverters. The inputs of each switching block are the outputs of the respective flux controller, torque controller, resultant time flux controller and sector information of the respective flux. For example, inputs to the optimal switching block 1 are T,F1,F_{res_t} and R1(N) (Fig.15).

When there is a torque demand (T=1), it is required to rotate $\vec{\Psi}_{res}$ to increase the angle between $\vec{\Psi}_{res}$ and $\vec{\Psi}_r$. $\vec{\Psi}_{res}$ is rotated in counter clock wise direction either by rotating $\vec{\Psi}_{s1}$ or $\vec{\Psi}_{s2}$. When θ exceeds the set value, then $\vec{\Psi}_{s1}$ is rotated and $\vec{\Psi}_{s2}$ is stopped (Fig.16). Similarly when θ is less than the set value $\vec{\Psi}_{s2}$ is rotated and $\vec{\Psi}_{s1}$ is stopped (Fig.17). Controlling in this way at all instants of time, the angle between the individual fluxes is maintained at thirty-degree. Magnitudes of individual fluxes are also kept constant by the individual flux controllers. Hence the magnitude of resultant flux is controlled and torque demand is also met. When there is no torque demand both the fluxes are stopped.

Switching states for both the inverters are given in table2a and table 2b.

Advantage: a) Line currents are free from 5th and 7th harmonic components.b) Torque ripple is lesser in magnitude. At any instant of time at most one inverter is switched to an active vector and other one is switched to zero vector. So individual torques generated by the inverters are varying in opposite phase. When one inverter is switched to increase the torque, other one causes to reduce it. Due to instantaneous individual torque ripple cancellation; the resultant torque ripple is lesser in magnitude than conventional three-phase DTC.

Disadvantage: At any instant of time only one inverter is switched to an active vector. It is not possible to use the voltage vectors from outer two polygons of resultant voltage vectors of SPIM drive (Fig.3). So the resultant applied voltage to the machine is less in for a fixed DC bus voltage. So the machine cannot run at a higher speed at rated flux. The maximum speed it can attain is half the rated speed.

Fres_t	F1	T	R'(1)	R'(2)	R'(3)	R'(4)	R'(5)	R'(6)
1	1	1	2'	3'	4'	5'	6'	1'
1	1	0	8'	7'	8'	7'	8'	7'
1	1	-1	8'	7'	8'	7'	8'	7'
1	0	1	3'	4'	5'	6'	1'	2'
1	0	0	7'	8'	7'	8'	7'	8'
1	0	-1	7'	8'	7'	8'	7'	8'
0	1	1	8'	7'	8'	7'	8'	7'
0	1	0	8'	7'	8'	7'	8'	7'
0	1	-1	6'	1'	2'	3'	4'	5'
0	0	1	7'	8'	7'	8'	7'	8'
0	0	0	7'	8'	7'	8'	7'	8'
0	0	-1	5'	6'	1'	2'	3'	4'

Table 2a (Inverter 1)

Fres_t	F2	T	R(1)	R(2)	R(3)	R(4)	R(5)	R(6)
1	1	1	8	7	8	7	8	7
1	1	0	8	7	8	7	8	7
1	1	-1	6	1	2	3	4	5
1	0	1	7	8	7	8	7	8
1	0	0	7	8	7	8	7	8
1	0	-1	5	6	1	2	3	4
0	1	1	2	3	4	5	6	1
0	1	0	8	7	8	7	8	7
0	1	-1	8	7	8	7	8	7
0	0	1	3	4	5	6	1	2
0	0	0	7	8	7	8	7	8
0	0	-1	7	8	7	8	7	8

Table 2b (Inverter 2)

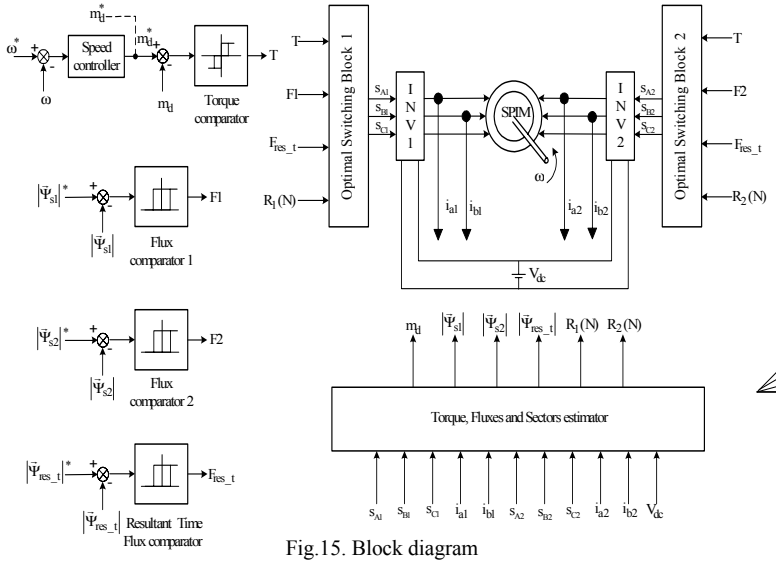

Fig.15. Block diagram

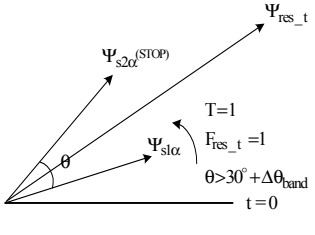

Fig.16.a. Time phasor

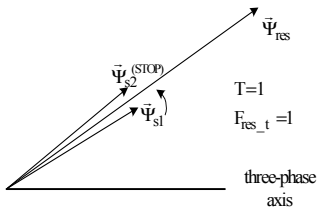

Fig.16.b.Space phasor

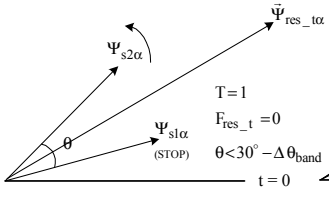

Fig.17.a. Time phasor

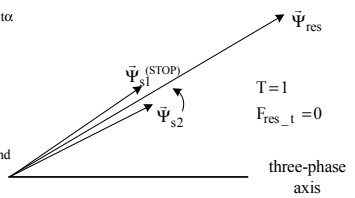

Fig.17.b.Space phasor

Experimental results: DC bus: 200V, No load, 300 rpm

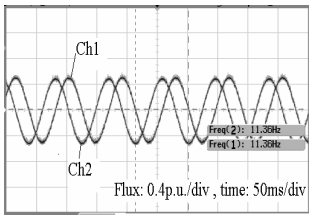

Fig.18.Ch1 : $\Psi_{s\beta 1}$ Ch2 : $\Psi_{s\alpha 1}$

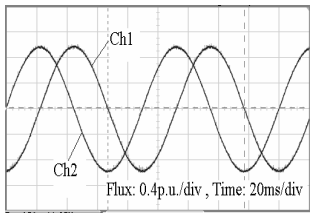

Fig.19.Ch1 : $\Psi_{res\beta}$ Ch2 : $\Psi_{res\alpha}$

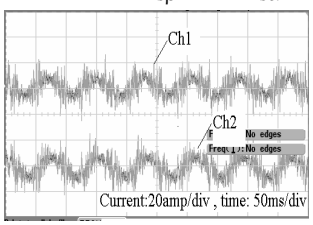

Fig.20.Ch1 : i_{s_a2} Ch2 : i_{s_a1}

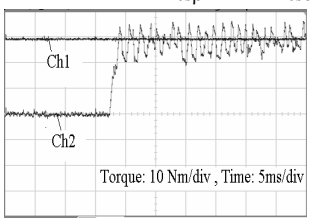

Fig.21. Ch1 : m_d^* Ch2 : m_d

VIII. INDIVIDUAL FLUX CONTROL ALGORITHM #02

Both the inverters have to be switched to active vectors simultaneously to run the machine at rated speed with rated DC bus voltage. In this algorithm, it is proposed to rotate both the fluxes simultaneously, keeping the magnitude of resultant flux constant at its reference value. To achieve this a three-level hysteresis controller with dead-zone is used as angle controller. The rest of the controllers remain the same as in Algorithm #01. When angle between the components of fluxes is within twenty to forty degrees, both of them are rotated keeping their magnitudes constant. When the angle exceeds beyond the set values, one of them is rotated and the other one is stopped to bring back the angle towards thirty degrees, similar to Algorithm #01.

Angle Controller:

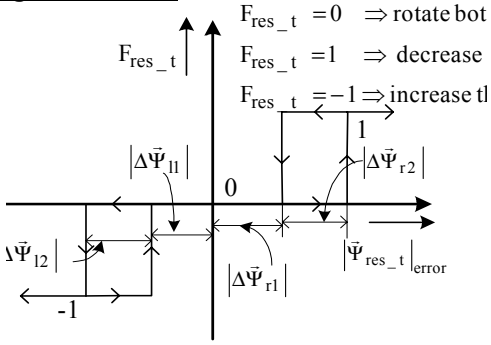

Fig.22. Angle controller

The different bands for angle controller are adjusted in such a way, that most of the time both the individual fluxes are rotated [4].

Optimal switching logic: Similar to Algorithm #01, there are two independent switching blocks for Inverter-1 and Inverter-2 respectively. As long as the output of F_{res_t} remains zero, both the individual fluxes are rotated as in three-phase DTC. When F_{res_t} = 1 or –1, then angle correcting action is taken, same as Algorithm #01 (Fig.16&17). Switching table for this method includes F_{res_t}= 0 state. In this state, switching table for both the inverters are same as conventional three-phase DTC[1] (table 3.a& 3.b). For F_{res_t} =1 and –1 state switching tables remain the same as algorithm #01(table 3.a &3.b).

Advantage: a) Rated speed of the machine is achieved.

Disadvantage: a) Torque ripple is high compared to Algorithm #01. b) Angle between the individual fluxes is not corrected during F_{res_t}=0 state.

Fres_t	F1	T	R'(N) N=1,2,…,6
1	1, 0	1, 0, -1	Same as table2.a.
0	1, 0	1, 0, -1	Same as 3-ϕ DTC [1].

Table 3.a. (Inverter1)

Fres_t	F2	T	R(N) N=1,2,…,6
1	1, 0	1, 0, -1	Same as table2.b.
0	1, 0	1, 0, -1	Same as 3-ϕ DTC [1].

Table 3.b. (Inverter2)

Experimental Results: DC Bus:250V, Machine speed:1000 r.p.m.,1.6KW load.

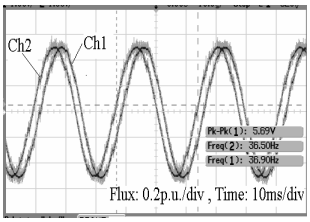

Fig.23.Ch1 : $\Psi_{s\alpha 1}$ Ch2 : $\Psi_{s\alpha 2}$

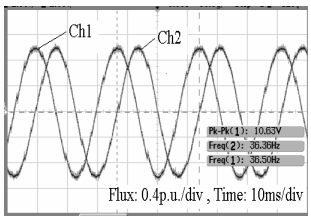

Fig.24.Ch1 : $\Psi_{res\alpha}$ Ch2 : $\Psi_{res\beta}$

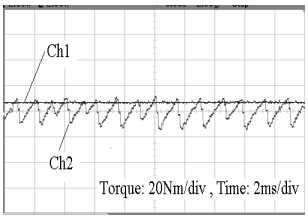

Fig.25.Ch1 : m_d^* Ch2 : m_d

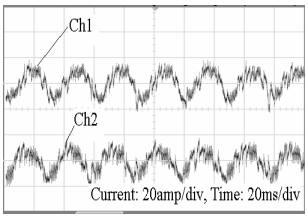

Fig.26.Ch1 : i_{s_a1} Ch2 : i_{s_a2}

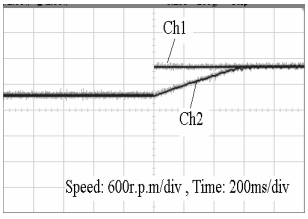

Fig.27.Ch1 : ω^* Ch2 : ω

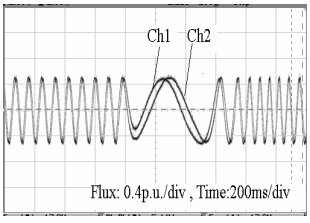

Fig.28.Fluxes during speed reversal Ch1 : $\Psi_{s\alpha 1}$ Ch2 : $\Psi_{s\alpha 2}$

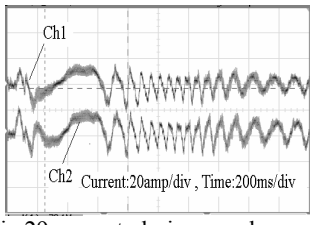

Fig.29. currents during speed reversal

Ch1 : i_{sa1} Ch2 : i_{sa2}

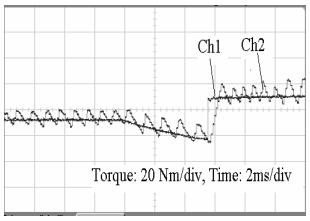

Fig.30. torque during speed reversal

Ch1 : m_d^* Ch2 : m_d

IX. INDIVIDUAL FLUX CONTROL ALGORITHM #03

Algorithm #03 tries to solve the problem faced in Algorithm #02. Torque ripple is considerably reduced in this algorithm. Angle between the components of individual fluxes are controlled most of the time. During F_{res_t} = 0 condition, angle correction is not taken care of in Algorithm #02. So both the fluxes move independently. But in this Algorithm, during F_{res_t} = 0 state, angle is corrected.

Active vectors are selected to increase the torque in anticlockwise and clockwise direction during T=1and T=-1 states respectively. During T=0 state, that is when decrease in torque is required, zero vectors are applied in conventional three-phase DTC and all above split-phase control algorithms. These switching patterns will give rise to torque ripple. The nature of the torque ripple varies at different speed ranges. For positive torque at a low speed, the rising edge of the torque ripple has a steeper slope than its falling edge. But at a higher speed, falling edge of the torque ripple has a steeper slope than the rising edge. Such variation in the nature of the torque ripple is due to different relative velocities of stator flux and rotor flux at different speeds (Fig.31.a).

In all the previous algorithms, during T=0 state, zero vectors are applied to both the inverters. So at a higher speed the torque ripple is high, due to drastic fall of individual torques contributed by both the inverters. In this method, to reduce the torque ripple, during T=0 state, zero vectors are applied to one of the inverters and active vectors are applied to the other inverter. Due to steeper slope of falling edge of torque ripple compared to the rising edge, the resultant torque is reduced to fulfill the command of T=0 state, but with a reduced slope (Fig.31.b).

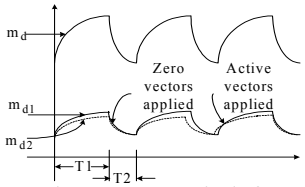

Fig. 31.a. Torque ripple for Algorithm #02

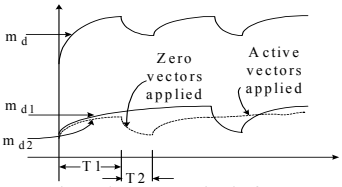

Fig.31.b. Torque ripple for Algorithm #03

Controllers: The controllers for individual fluxes and angle are remain the same as in Algorithm#03. Along with these controllers a four-level torque controller and a two-level torque ripple controller are used to select the appropriate inverter for applying zero vectors during T=+1/2 & T=-1/2 state.

Torque Ripple Controller: This controller is active during T=+1/2 and –1/2 state. This is a two-level ON-OFF controller. Output of the torque ripple controller (F_{TR}) decides, whether the angle between individual fluxes are more than or less than thirty degrees (Fig.32).

Torque Controller: T=0 state of a conventional torque controller is separated into two states. They are defined as T=+1/2 and T=-1/2 state. The upper half of the torque controller is used for positive torque demand. The lower half of the torque controller is used for negative torque demand (Fig.33).

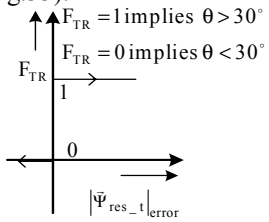

Fig.32. Torque Ripple Controller

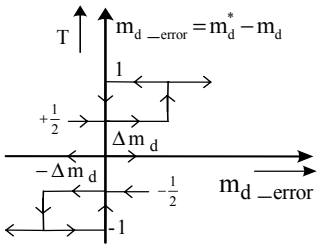

Fig.33. Torque Controller

X. OPTIMAL SWITCHING LOGIC

During T=1 and T=-1 state, the switching logic remains the same as in Algorithm #03. During T=+1/2 and T=-1/2 states, both the inverters are not switched to zero vectors. One of them is kept at active state to reduce the resultant torque ripple and to correct the phase angle between the components of individual fluxes. Output of the torque ripple controller(F_{TR}) decides the inverter to be switched at active state. For example, when T=+1/2 and F_{TR}=1, only $\bar{\Psi}_{s1}$ is rotated (Fig.34.a). Similarly, when T=+1/2 and F_{TR}=0, $\bar{\Psi}_{s2}$only is rotated (Fig.34.b).

Switching table for this method is given in table.4.a and 4.b.

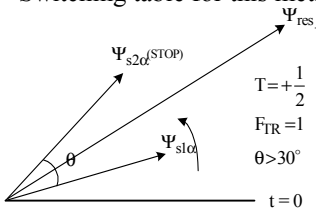

Fig.34.a. Phasor diagram.

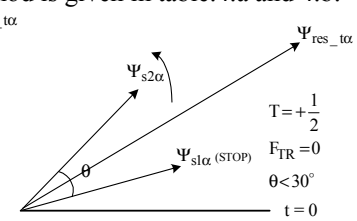

Fig.34.b. Phasor diagram

Advantage: **a.** Torque ripple is considerably reduced. The ripple is lesser in magnitude compared to three-phase DTC scheme. In three-phase DTC scheme, during T=0 state, stator flux is stopped. At a higher speed, rotor flux moves fast and the rate of decrease in the angle between them is also fast. Therefore the torque ripple is high. But in this method during T=0 state, resultant stator flux is also rotated but at a slower rate compared to the rotor flux. So torque ripple magnitude is lesser**. b.** Angle between the individual fluxes is corrected during T=0 state. **c.** Fluxes are smoother.

Disadvantage: **a.** At lower speed this algorithm cannot work. Rate of rise of the torque is faster than the rate of fall of the torque. Therefore if one of the inverter is switched to active state during T=0, resultant torque will increase. So the machine is started with Algorithm #02. After a certain speed (350 rpm) it is switched over to Algorithm #03.

F_{TR}		F_{rest}		F1		T	R'(N) N=1,2,3,4,5,6		
1,0		1,0,-1		1,0		1,-1	Same as table 3.a		
F_{TR}	F_{rest}	F1	T	R'(1)	R'(2)	R'(3)	R'(4)	R'(5)	R'(6)
0	0	1	+1/2	8'	7'	8'	7'	8'	7'
0	0	1	-1/2	6'	1'	2'	3'	4'	5'
0	0	0	+1/2	7'	8'	7'	8'	7'	8'
0	0	0	-1/2	5'	6'	1'	2'	3'	4'
0	-1	1	+1/2	7'	8'	7'	8'	7'	8'
0	-1	1	-1/2	6'	1'	2'	3'	4'	5'
0	-1	0	+1/2	8'	7'	8'	7'	8'	7'
0	-1	0	-1/2	5'	6'	1'	2'	3'	4'
1	1	1	+1/2	2'	3'	4'	5'	6'	1'
1	1	1	-1/2	8'	7'	8'	7'	8'	7'
1	1	0	+1/2	3'	4'	5'	6'	1'	2'
1	1	0	-1/2	7'	8'	7'	8'	7'	8'
1	0	1	+1/2	2'	3'	4'	5'	6'	1'
1	0	1	-1/2	8'	7'	8'	7'	8'	7'
1	0	0	+1/2	3'	4'	5'	6'	1'	2'
1	0	0	-1/2	7'	8'	7'	8'	7'	8'

Table 4.a (Inverter1)

F_{TR}		F_{rest}		F2		T	R(N) N=1,2,3,4,5,6		
1,0		1,0,-1		1,0		1,-1	Same as table 3.b		
F_{TR}	F_{rest}	F2	T	R(1)	R(2)	R(3)	R(4)	R(5)	R(6)
0	0	1	+1/2	2	3	4	5	6	1
0	0	1	-1/2	8	7	8	7	8	7
0	0	0	+1/2	3	4	5	6	1	2
0	0	0	-1/2	7	8	7	8	7	8
0	-1	1	+1/2	2	3	4	5	6	1
0	-1	1	-1/2	8	7	8	7	8	7
0	-1	0	+1/2	3	4	5	6	1	2
0	-1	0	-1/2	7	8	7	8	7	8
1	1	1	+1/2	8	7	8	7	8	7
1	1	1	-1/2	6	1	2	3	4	5
1	1	0	+1/2	8	7	8	7	8	7
1	1	0	-1/2	5	6	1	2	3	4
1	0	1	+1/2	8	7	8	7	8	7
1	0	1	-1/2	6	1	2	3	4	5
1	0	0	+1/2	7	8	7	8	7	8
1	0	0	-1/2	5	6	1	2	3	4

Table 4.b (Inverter2)

Experimental results: DC Bus:200V , Machine speed = 630 r.p.m., 1KW load.

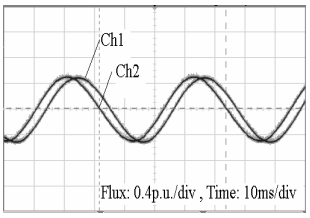

Fig.35.Ch1 : $\Psi_{s\alpha 1}$ Ch2 : $\Psi_{s\alpha 2}$

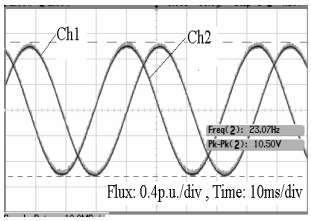

Fig.36.Ch1 : $\Psi_{res\beta}$ Ch2 : $\Psi_{res\alpha}$

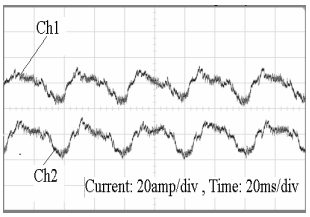

Fig.37.Ch1 : i_{s_a2} Ch2 : i_{s_a1}

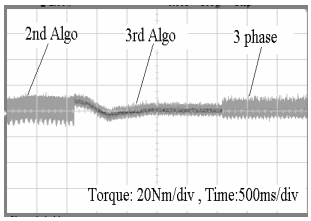

Fig.38.Torque transients at no load

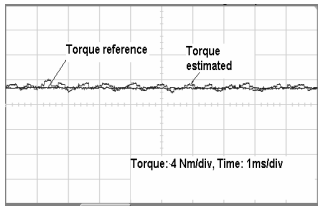

Fig.39.Torque estimated and torque reference

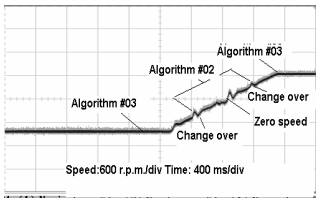

Fig.40.Speed reversal :
$-350 < \omega < 350$: Algorithm #02
$\omega < -350$ & $\omega > 350$: Algorithm #03

X.CONCLUSION

In this paper SPIM DTC schemes are established. It is found that, machine can run the full speed range along with speed reversal with reduced torque ripple with Algorithm #03 along with Algorithm #02.In lower speed range, machine is operated with Algorithm #02 and higher speed range machine is operated with Algorithm #03. A smooth transition, between these two algorithms is implemented.

Implementation was carried out on fixed point DSP processor (TMS320C50). Sampling time is 110micro seconds. 1000 volts, 50 amps, IGBTs (MG50BZ100) are used for the inverters. A 6KW SPIM coupled with a DC machine is used as a test set up.

REFERENCES

[1] Isao Takahashi and Toshihiko Noguchi, "A New Quick Response and High Effiency Control Strategy of an Induction Motor ", *IEEE Transaction on Industry Applications,* Vol-25, No.5, pp.820-827, September/October 1986.

[2] K.Gopakumar, V.T.Ranganathan, S.R.Bhat, "Split-phase Induction Motor Operation from PWM Voltage Source Inverter", *IEEE transaction on Industry Applications,* Vol.29, No.5, pp.927-932, September/October 1993.

[3]Kevin D.Hurst, Thomas G. Habetler, Giovanni Griva, Francesco Profumo, " Zero-Speed Tacholess IM Torque Control: Simply a Matter of Stator Voltage Integration", *IEEE Transaction on Industry Applications,* Vol.34, No.4, pp. 790-795, July/August 1998.

[4] Kamalesh Hatua, "Direct Torque Control Schemes for Split-Phase Induction Machine", M.Sc.(Engg.) Thesis,IISc. Bangalore-12, November-2003.